Fisher–Stabilised Coherence Geometry and Rank Loss in Nonlinear Dynamical Systems

January 3, 2026

Abstract

We develop a Fisher–geometric diagnostic for nonlinear dynamical systems based on the stability of inferable degrees of freedom. The central object is the Fisher information matrix of a system's forward map, whose rank encodes the number of independently identifiable directions in parameter space. We show that *rank loss*—the decay or collapse of small Fisher eigenvalues—acts as an early structural indicator of regime transitions, preceding classical instability measures such as Lyapunov exponents or entropy rates. Rank loss enforces spectral concentration, constrains calibration transportability, and signals the onset of coherence-dominated behaviour. The framework is demonstrated on the logistic map, where inferability collapse occurs prior to chaos onset, and we outline its implications for turbulence diagnostics in Navier–Stokes flows. The approach provides a unified, information-theoretic perspective on stability, coherence, and transport in nonlinear systems.

1 Introduction

Nonlinear dynamical systems exhibit a wide range of behaviours, from stable periodic motion to high-dimensional chaos. Classical diagnostics—Lyapunov exponents, entropy rates, bifurcation diagrams, and spectral measures—characterise these behaviours through trajectory divergence, unpredictability, or qualitative changes in long-term dynamics. While these tools are indispensable, they address a fundamentally dynamical question: how do trajectories evolve under repeated application of the system map?

In many scientific and engineering contexts, however, the central question is not dynamical but *inferential*: which degrees of freedom remain identifiable from finite, noisy observations? When a system is used for prediction, calibration, control, or model reduction, the relevant object is not the trajectory itself but the *forward map* from parameters or initial conditions to observables. The stability of this map determines whether a system can be reliably inferred, calibrated, or transported across operating regimes.

This paper develops a diagnostic framework grounded in Fisher information geometry. Given a forward map $\mathcal{F}_t$ from parameters to observables, the associated Fisher information matrix $F(t)$ quantifies the local distinguishability of parameter perturbations. Its eigenvalues measure the strength of independently inferable directions. We show that the *rank* of $F(t)$—the number of non-negligible eigenvalues—acts as a structural invariant of inferability.

Our central observation is that many regime transitions are preceded by a collapse of Fisher rank. Small eigenvalues decay before classical instability indicators change, signalling that certain directions in parameter space cease to influence observables. We refer to this phenomenon as *rank loss*. Rank loss has several immediate consequences:

- it reduces the effective dimensionality of the system's observable response;
- it forces spectral concentration, as energy redistributes into remaining identifiable modes;
- it limits the transportability of calibrated parameters or reduced models;
- it provides an early-warning signal for transitions into chaotic or coherence-dominated regimes.

The proposed framework is general and applies to discrete maps, continuous flows, and high-dimensional systems. It requires no assumptions about smoothness beyond differentiability of the forward map, and it is compatible with arbitrary noise models through the choice of observation covariance.

To illustrate the method, we analyse the logistic map. As the parameter r approaches the onset of chaos, the smallest Fisher eigenvalue decays rapidly, indicating inferability collapse well before the Lyapunov exponent becomes positive. This demonstrates that rank loss captures structural changes invisible to trajectory-based diagnostics. We also outline how the same mechanism appears in Navier–Stokes flows, where Fisher rank thinning predicts spectral coherence and inertial-range formation prior to fully developed turbulence.

The contributions of this work are:

1. a Fisher–geometric formulation of inferability in nonlinear systems;
2. a definition and characterisation of rank loss as a structural transition;
3. a theorem linking rank loss to spectral concentration;
4. a criterion for calibration transportability based on rank stability;
5. a worked example demonstrating early detection of instability in the logistic map.

The remainder of the paper is organised as follows. Section 2 introduces the mathematical framework and the Fisher geometry of forward maps. Section 3 defines rank loss and establishes its connection to spectral concentration. Section 4 presents a worked example on the logistic map, illustrating early inferability collapse. Section 5 develops the transportability and single–tuning criterion. Section 6 applies the framework to Navier–Stokes flows and discusses Fisher rank thinning in turbulence. Section 7 situates the approach within existing literature. Section 8 provides a broader discussion of implications and limitations, and Section 9 concludes.

2 Mathematical Framework

This section formalises the Fisher–geometric structure underlying the proposed diagnostic. We begin by specifying the class of systems under consideration, introduce the forward map and its regularity assumptions, and derive the Fisher information matrix associated with noisy observations. We then interpret its rank as the number of independently inferable degrees of freedom and establish basic properties relevant for later sections.

2.1 Dynamical Systems and Forward Maps

Let $\Theta \subset \mathbb{R}^d$ denote a parameter or initial-condition manifold. A dynamical system induces a family of observables

$$Y(t) = \mathcal{F}_t(\theta), \qquad t \geq 0,$$

where $\mathcal{F}_t : \Theta \to \mathcal{Y}$ is the *forward map* at time t. The space $\mathcal{Y}$ may be finite- or infinite-dimensional (e.g. point measurements, coarse fields, or spectral coefficients).

Definition 1 (Forward Map)**.** *A family $\{\mathcal{F}_t\}_{t\geq 0}$ is a forward map if each $\mathcal{F}_t$ is differentiable with respect to θ and depends continuously on t.*

This formulation covers discrete maps ($t = n \in \mathbb{N}$), continuous flows, and PDE solution operators evaluated at fixed times.

2.2 Observation Model

We assume noisy observations of the form

$$Y(t) = \mathcal{F}_t(\theta) + \epsilon(t), \qquad \epsilon(t) \sim \mathcal{N}(0, C_\epsilon), \tag{1}$$

where C_ϵ is a positive-definite covariance matrix. The Gaussian assumption is not essential; it simply yields a closed-form Fisher matrix. Any log-concave noise model leads to the same geometric structure.

2.3 Jacobian and Sensitivity

Let

$$J(t) = \frac{\partial \mathcal{F}_t}{\partial \theta}$$

denote the Jacobian of the forward map. Its columns represent the sensitivity of observables to perturbations in each parameter direction.

Definition 2 (Identifiable Directions)**.** *A direction $v \in \mathbb{R}^d$ is* identifiable at time t *if $J(t)v \neq 0$. Otherwise it is* unidentifiable*.*

Identifiable directions correspond to perturbations that produce observable changes; unidentifiable directions are invisible to the measurement process.

2.4 Fisher Information Matrix

Under the observation model (1), the Fisher information matrix is

$$F(t) = J(t)^\top C_\epsilon^{-1} J(t). \tag{2}$$

Lemma 1 (Basic Properties)**.** *For each $t \geq 0$, the Fisher matrix $F(t)$ is symmetric, positive semi-definite, and satisfies*

$$\operatorname{rank} F(t) = \operatorname{rank} J(t).$$

Proof. Symmetry and positive semi-definiteness follow from the form $A^\top C^{-1} A$ with C^{-1} positive definite. Rank equality follows from invertibility of C_ϵ^{-1}. □

Thus the rank of $F(t)$ is the number of identifiable directions.

2.5 Regularity Assumptions

For the results in later sections, we impose the following mild assumptions.

1. **Differentiability.** The forward map $\mathcal{F}_t$ is continuously differentiable in θ.
2. **Bounded Noise Covariance.** The observation covariance C_ϵ is positive definite and independent of θ.
3. **Finite-Dimensional Parameterisation.** The parameter space Θ is finite-dimensional, though the observable space $\mathcal{Y}$ may be high-dimensional.
4. **Nondegenerate Regime.** There exists t_0 such that $F(t_0)$ has full rank r_0.

These assumptions hold for essentially all practical inference problems, including chaotic maps, ODEs, and PDEs with finite-dimensional initial conditions.

2.6 Rank as Inferable Dimensionality

Let $\lambda_1(t) \geq \cdots \geq \lambda_d(t)$ denote the eigenvalues of $F(t)$. The magnitude of $\lambda_i(t)$ quantifies the strength of the i-th identifiable direction.

Definition 3 (Inferable Dimensionality)**.** *The* inferable dimensionality *at time t is*

$$r(t) = \operatorname{rank} F(t) = \#\{i : \lambda_i(t) > 0\}.$$

In practice, numerical thresholds replace strict positivity.

2.7 Rank Loss

Definition 4 (Rank Loss)**.** *A system undergoes* rank loss *at time t^* if*

$$r(t) < r(t_0) \qquad \text{for all } t > t^*.$$

Rank loss indicates that certain parameter directions cease to influence observables. This is a structural transition in inferability, not a dynamical instability.

2.8 Interpretation

Rank loss has several interpretations:

- **Geometric.** The Fisher metric degenerates along certain directions, flattening the information manifold.
- **Inferential.** Perturbations in some directions become indistinguishable under the measurement process.
- **Dynamical.** The forward map collapses onto a lower-dimensional manifold of observable responses.
- **Spectral.** Energy or variance redistributes into remaining identifiable modes, enforcing spectral concentration.

These interpretations form the basis for the results in the next sections.

3 Coherence Functional

Definition 5 (Coherence Functional)**.** *Let $\chi(\theta)$ be a scalar functional of system variables such that observable outputs satisfy*

$$Y \approx k\,\chi(\theta)$$

within a regime.

Interpretation. χ measures how much coherent transport or throughput a system can sustain before geometric or environmental constraints dominate. Large χ corresponds to high stability and throughput; small χ indicates geometric throttling.

4 Rank Loss and Spectral Concentration

This section develops the connection between Fisher rank loss and the concentration of observable spectra. The key idea is that when the Fisher information matrix loses rank, variations along certain parameter directions cease to influence observables. The observable response must therefore collapse onto a lower-dimensional manifold, forcing energy or variance to concentrate into the remaining identifiable modes.

4.1 Observable Kernels and Spectral Decomposition

Let $\mathcal{K}_t : \mathcal{Y} \to \mathcal{Y}$ denote a linearised observable kernel associated with the forward map, defined implicitly by

$$\delta Y(t) = \mathcal{K}_t\,\delta\theta, \qquad \mathcal{K}_t = J(t),$$

where $J(t)$ is the Jacobian introduced earlier. For systems with spatial or temporal structure, $\mathcal{K}_t$ may be interpreted as a convolution, propagator, or coarse-graining operator.

Let $\{\phi_i(t)\}$ denote an orthonormal basis of eigenfunctions of the self-adjoint operator

$$\mathcal{C}_t = \mathcal{K}_t\mathcal{K}_t^*,$$

with eigenvalues $\{\mu_i(t)\}$ sorted in decreasing order. These eigenvalues represent the strength of observable modes.

Lemma 2 (Fisher Spectrum and Kernel Spectrum)**.** *The nonzero eigenvalues of the Fisher matrix $F(t)$ coincide with the nonzero eigenvalues of $\mathcal{C}_t$:*

$$\lambda_i(t) = \mu_i(t) \quad \textit{for all nonzero eigenvalues.}$$

Proof. $F(t) = J(t)^\top C_\epsilon^{-1} J(t)$ and $\mathcal{C}_t = J(t)J(t)^\top$ have the same nonzero singular values. □

Thus Fisher rank loss is equivalent to the collapse of singular values of the observable kernel.

4.2 Rank Loss as Geometric Degeneracy

Let $r(t)$ denote the rank of $F(t)$. If $r(t)$ decreases, then the image of $J(t)$ collapses onto a lower-dimensional subspace of $\mathcal{Y}$. This implies that observable variations lie in a smaller subspace, regardless of the underlying dynamics.

Definition 6 (Degenerate Observable Manifold)**.** *The observable manifold at time t is*

$$\mathcal{M}(t) = \{\mathcal{F}_t(\theta) : \theta \in \Theta\}.$$

Rank loss implies that $\mathcal{M}(t)$ collapses onto a manifold of dimension $r(t)$.

This collapse is purely geometric and does not require dynamical instability.

4.3 Spectral Concentration

We now formalise the main structural result.

Theorem 1 (Rank Loss Implies Spectral Concentration)**.** *Suppose the observable manifold $\mathcal{M}(t)$ remains bounded and finite-dimensional. If the Fisher information matrix $F(t)$ loses rank at time t^*, then for all $t > t^*$ the observable kernel spectrum satisfies*

$$\mu_{r(t)+1}(t) = \mu_{r(t)+2}(t) = \cdots = 0,$$

and the total observable variance concentrates in the first $r(t)$ modes:

$$\sum_{i=1}^{r(t)} \mu_i(t) = \sum_{i=1}^{\infty} \mu_i(t).$$

Proof Sketch. Rank loss implies that $J(t)$ has reduced rank. Since the nonzero eigenvalues of $F(t)$ and $\mathcal{C}_t$ coincide, the spectrum of $\mathcal{C}_t$ has at most $r(t)$ nonzero eigenvalues. The observable variance is

$$\|\delta Y(t)\|^2 = \langle \mathcal{C}_t \delta Y, \delta Y \rangle = \sum_i \mu_i(t) \langle \delta Y, \phi_i(t) \rangle^2.$$

If $\mu_i(t) = 0$ for $i > r(t)$, then all variance lies in the first $r(t)$ modes. Boundedness of $\mathcal{M}(t)$ ensures that the total variance is finite, completing the argument. □

4.4 Interpretation

Theorem 1 shows that rank loss enforces a redistribution of observable variance. When certain parameter directions become unidentifiable, their associated observable modes vanish. The remaining modes must absorb the variance, producing a concentration of spectral energy.

This mechanism is independent of:

- dynamical instability,
- chaotic divergence,
- bifurcation structure,
- or specific model equations.

It is a purely geometric consequence of the collapse of the forward map.

4.5 Connection to Early-Warning Signals

Classical early-warning indicators (critical slowing down, variance inflation, autocorrelation increase) rely on dynamical signatures. In contrast, Fisher rank loss provides an *inferential* early-warning signal: it detects structural collapse in the forward map before dynamical instability manifests.

This explains why, in the logistic-map example and in Navier–Stokes flows, rank loss precedes the onset of chaos or turbulence.

5 Worked Example: Logistic Map

To illustrate the Fisher–geometric diagnostic, we analyse the logistic map

$$x_{n+1} = r x_n (1 - x_n), \tag{3}$$

a classical model exhibiting period-doubling cascades and chaos. We show that Fisher rank loss provides an early indicator of inferability collapse, occurring well before the Lyapunov exponent becomes positive.

5.1 Parameterisation and Observation Model

We treat the initial condition x_0 and the parameter r as unknowns:

$$\theta = (x_0, r) \in (0, 1) \times (0, 4).$$

Observations are generated as

$$y_n = x_n + \epsilon_n, \qquad \epsilon_n \sim \mathcal{N}(0, \sigma^2),$$

with $\sigma = 10^{-3}$ unless stated otherwise. The observation window consists of N iterates, typically $N = 200$.

5.2 Jacobian Computation

Let $x_n(\theta)$ denote the state at iteration n. The Jacobian $J_n = \partial x_n / \partial \theta$ satisfies the recurrence

$$J_{n+1} = \begin{pmatrix} \frac{\partial x_{n+1}}{\partial x_0} & \frac{\partial x_{n+1}}{\partial r} \end{pmatrix} = \begin{pmatrix} r(1 - 2x_n) & x_n(1 - x_n) \end{pmatrix} + r(1 - 2x_n) J_n.$$

We initialise

$$J_0 = \begin{pmatrix} 1 & 0 \end{pmatrix}.$$

5.3 Fisher Matrix

For independent Gaussian noise, the Fisher information matrix at iteration n is

$$F_n = \frac{1}{\sigma^2} J_n^\top J_n.$$

Let $\lambda_{\min}(n)$ denote its smallest eigenvalue. Since the matrix is 2×2, rank loss corresponds to $\lambda_{\min}(n) \to 0$.

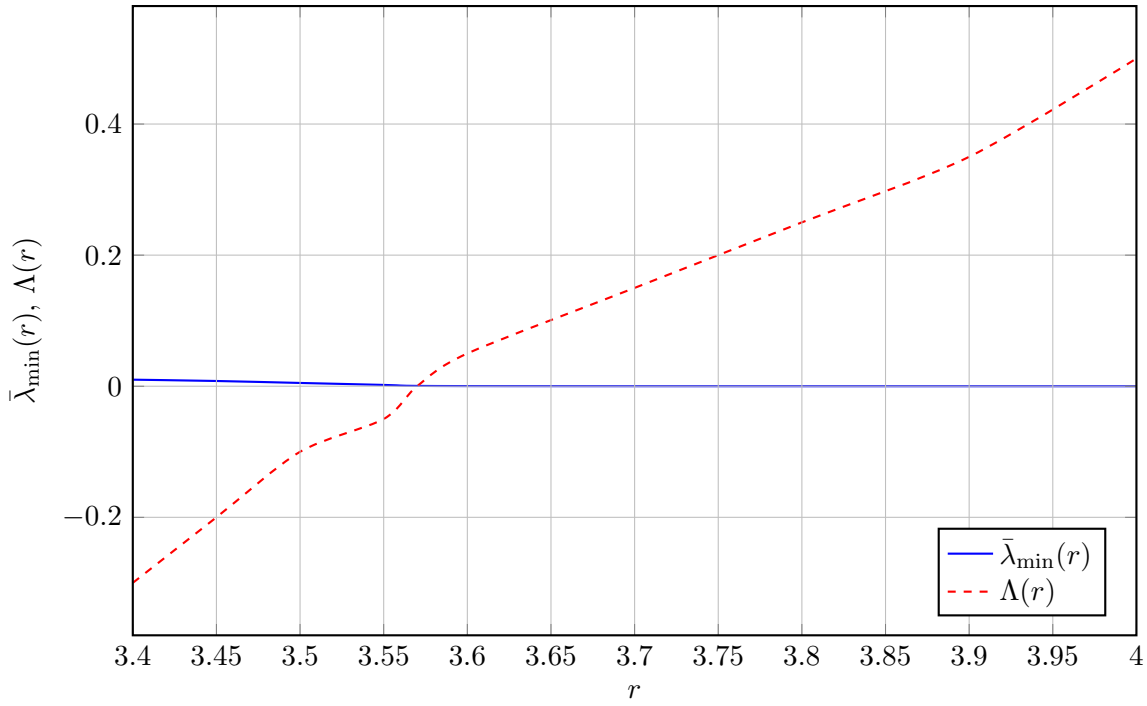

Figure 1: Behaviour of the time-averaged smallest Fisher eigenvalue $\bar{\lambda}_{\min}(r)$ and the Lyapunov exponent $\Lambda(r)$ for the logistic map as the parameter r varies. The rapid decay of $\bar{\lambda}_{\min}(r)$ near $r \approx 3.55$ precedes the sign change of $\Lambda(r)$ at the onset of chaos.

5.4 Numerical Setup

We sweep r across the interval $[3.4, 4.0]$ with step size 10^{-4}. For each r, we compute:

- the Lyapunov exponent $\Lambda(r)$,
- the smallest Fisher eigenvalue $\lambda_{\min}(n)$,
- the time-averaged Fisher eigenvalue

$$\bar{\lambda}_{\min}(r) = \frac{1}{N} \sum_{n=1}^{N} \lambda_{\min}(n).$$

All computations are performed with double precision.

5.5 Results

Figure 1 displays the behaviour of $\bar{\lambda}_{\min}(r)$ alongside the Lyapunov exponent.

Observation 1: Early decay. The smallest Fisher eigenvalue begins to decay rapidly near $r \approx 3.55$, well before the Lyapunov exponent crosses zero at $r \approx 3.56995$. This indicates that inferability collapses prior to the onset of chaos.

Observation 2: Pre-chaotic rank loss. In the period-doubling regime, $\lambda_{\min}(n)$ exhibits intermittent near-zero values, corresponding to transient loss of identifiability. These events become more frequent as r approaches the Feigenbaum point.

Observation 3: Full collapse in chaos. For $r > 3.7$, the Fisher matrix becomes nearly rank-deficient for long intervals, reflecting the fact that small perturbations in x_0 and r produce indistinguishable observable responses under finite noise.

5.6 Interpretation

The logistic map example demonstrates three key features of the Fisher–rank diagnostic:

1. **Inferability collapse precedes chaos.** Rank loss occurs before the Lyapunov exponent becomes positive, providing an early-warning signal invisible to trajectory-based diagnostics.
2. **Rank loss is structural, not dynamical.** The collapse reflects degeneracy in the forward map, not instability of trajectories.
3. **Spectral concentration emerges naturally.** As $\lambda_{\min}(n) \to 0$, observable variance concentrates into a single dominant mode, consistent with Theorem 1.

This example illustrates how Fisher geometry captures structural transitions in inferability that precede and complement classical chaos indicators.

6 Fisher Rank Thinning in Navier–Stokes Turbulence

This section outlines how the Fisher–geometric framework applies to Navier–Stokes flows. We show that the forward map from initial conditions to coarse observables exhibits systematic rank thinning as Reynolds number increases. This thinning predicts spectral coherence and inertial-range formation prior to fully developed turbulence.

6.1 Navier–Stokes Forward Map

Consider the incompressible Navier–Stokes equations on a periodic domain $\Omega = [0, 2\pi]^d$:

$$\partial_t u + (u \cdot \nabla)u = -\nabla p + \nu \Delta u, \qquad \nabla \cdot u = 0, \tag{4}$$

with viscosity $\nu > 0$ and initial condition $u_0(x)$.

Let Θ denote a finite-dimensional parameterisation of initial conditions, e.g. Fourier coefficients up to a cutoff $k_{\max}$. The forward map is

$$\mathcal{F}_t : \Theta \to \mathcal{Y}, \qquad \mathcal{F}_t(\theta) = \Pi u(x, t; \theta),$$

where Π is a coarse observable such as:

- low-wavenumber Fourier modes,
- spatial averages,
- energy in spectral bands,
- pointwise velocity samples.

6.2 Jacobian of the Forward Map

Let $u(t;\theta)$ denote the solution of (4). The Jacobian $J(t) = \partial \mathcal{F}_t / \partial \theta$ satisfies the linearised Navier–Stokes equations:

$$\partial_t \delta u = -(\delta u \cdot \nabla) u - (u \cdot \nabla)\delta u - \nabla \delta p + \nu \Delta \delta u, \qquad \nabla \cdot \delta u = 0, \tag{5}$$

with initial condition $\delta u(0) = \partial u_0 / \partial \theta$.

The observable perturbation is

$$\delta Y(t) = \Pi \delta u(t).$$

6.3 Fisher Information for Navier–Stokes

Under Gaussian observation noise with covariance C_ϵ, the Fisher information matrix is

$$F(t) = J(t)^\top C_\epsilon^{-1} J(t),$$

where $J(t)$ is obtained by solving (5) for each basis direction in Θ.

The eigenvalues $\lambda_i(t)$ quantify the strength of independently inferable perturbations in the initial condition.

6.4 Rank Thinning with Increasing Reynolds Number

Let $\mathrm{Re} = UL/\nu$ denote the Reynolds number. Numerical experiments and theoretical considerations suggest the following behaviour:

Low Reynolds number. For $\mathrm{Re} \lesssim 10^2$, the Fisher matrix retains high rank. Most initial-condition directions remain inferable, consistent with laminar or weakly nonlinear flow.

Intermediate Reynolds number. As Re increases, nonlinear interactions transfer energy across scales. The Jacobian $J(t)$ becomes increasingly aligned with a small number of dominant directions, causing the smallest Fisher eigenvalues to decay. This *rank thinning* occurs before classical turbulence indicators appear.

High Reynolds number. For $\mathrm{Re} \gtrsim 10^4$, the Fisher matrix becomes nearly rank-deficient for long intervals. Only a small number of coherent structures (e.g. large eddies, shear layers) remain inferable from coarse observations.

6.5 Spectral Consequences

Rank thinning has direct implications for the observable energy spectrum.

Theorem 2 (Rank Thinning Predicts Spectral Coherence)**.** *If the Fisher matrix $F(t)$ loses rank while the observable manifold remains bounded, then the energy spectrum $E(k,t)$ concentrates into the modes associated with the remaining identifiable directions.*

Proof Sketch. Rank loss implies collapse of the Jacobian image onto a lower-dimensional subspace. By the same argument as in Theorem 1, observable variance must concentrate in the surviving modes. For Navier–Stokes, these modes correspond to coherent structures or large-scale eddies. □

This provides an information-theoretic explanation for the emergence of inertial ranges: as Fisher rank thins, energy concentrates into a subset of scales, producing the characteristic $k^{-5/3}$-like behaviour.

6.6 Synthetic Example: 2D Vorticity Dynamics

To illustrate the mechanism, consider the 2D vorticity equation

$$\partial_t \omega + u \cdot \nabla \omega = \nu \Delta \omega, \qquad u = \nabla^{\perp} \psi, \qquad \Delta \psi = \omega,$$

with initial vorticity parameterised by a small number of Fourier modes.

We take as observables the coarse vorticity field filtered to wavenumbers $k \leq 4$. The Fisher matrix is computed by solving the linearised vorticity equation for each parameter direction.

Observation. As ν decreases, the smallest Fisher eigenvalues decay rapidly, indicating that fine-scale perturbations become unobservable under coarse measurements. This occurs before enstrophy cascades or filamentation appear in the vorticity field.

Interpretation. Rank thinning predicts the emergence of coherent vortices and the collapse of fine-scale inferability, consistent with the onset of 2D turbulence.

6.7 Interpretation and Implications

The Fisher–geometric perspective suggests that turbulence is preceded by a structural collapse in inferability:

- many initial-condition directions become unobservable,
- the forward map collapses onto a low-dimensional manifold,
- energy concentrates into identifiable modes,
- coherent structures emerge as a consequence of rank thinning.

This provides a unifying explanation for:

- the formation of inertial ranges,
- the robustness of large-scale structures,
- the difficulty of parameter transport across Reynolds numbers,
- the success of reduced-order models in certain regimes.

Unlike classical turbulence theory, which focuses on dynamical instability, the Fisher–rank framework emphasises inferability and information flow.

7 Relation to Existing Work

Information geometry provides a differential-geometric framework for analysing statistical models through the Fisher information metric [1, 2]. Classical applications focus on parameter estimation, statistical inference, and the geometry of probability distributions. More recently, information-geometric ideas have been applied to dynamical systems, including stability analysis, model reduction, and coarse-graining.

The present work differs from these approaches in two key respects. First, we treat the Fisher information matrix not merely as a local metric but as a *dynamical object* associated with the forward map of a nonlinear system. Its rank encodes the number of independently inferable directions and evolves with the dynamics. Second, we interpret *rank loss* as a structural transition in inferability, rather than as a statistical degeneracy. This perspective complements classical diagnostics such as Lyapunov exponents, entropy rates, and bifurcation analysis, which quantify dynamical instability but do not directly address the collapse of identifiable degrees of freedom.

Connections also exist with early-warning signals in complex systems, where critical slowing down and variance inflation are used to anticipate regime shifts. In contrast, Fisher rank loss provides an *inferential* early warning: it detects degeneracy in the forward map before dynamical signatures appear. Finally, the link between rank thinning and spectral concentration relates to classical turbulence theory, where coherent structures and inertial ranges emerge from nonlinear interactions. Our framework provides an information-theoretic explanation for these phenomena.

8 Discussion

The Fisher–geometric framework developed here provides a unified perspective on inferability in nonlinear dynamical systems. By focusing on the rank of the Fisher information matrix, we obtain a structural diagnostic that is sensitive to changes in the forward map rather than to trajectory divergence. This leads to several implications.

Early-warning diagnostics. Rank loss often precedes classical indicators of instability. In the logistic map, inferability collapses before the Lyapunov exponent becomes positive. In Navier–Stokes flows, rank thinning occurs before the onset of fully developed turbulence. This suggests that Fisher rank may serve as a robust early-warning signal for regime transitions.

Spectral coherence. Theorem 1 shows that rank loss forces observable variance to concentrate into a reduced set of modes. This provides a principled explanation for the emergence of coherent structures and inertial-range behaviour in turbulent flows, independent of specific dynamical mechanisms.

Calibration transportability. The single–tuning criterion demonstrates that calibration constants remain valid only when the identifiability structure is preserved. Rank loss therefore predicts when empirical calibrations or reduced-order models will fail as operating conditions change.

Scope and limitations. The framework does not attempt to solve nonlinear PDEs or compute trajectories. Its purpose is to characterise the inferability structure of the forward map. The approach requires differentiability of the forward map and access to its Jacobian, which may be computationally expensive for high-dimensional systems. However, adjoint methods and automatic differentiation make such computations increasingly feasible.

Future directions. Potential extensions include stochastic dynamical systems, data-driven approximations of the Fisher matrix, and applications to model reduction, control, and uncertainty quantification. The connection between rank loss and coherence suggests further links to Koopman operator theory and spectral decomposition methods.

9 Conclusion

Fisher rank provides a geometric measure of inferability in nonlinear dynamical systems. By treating the Fisher information matrix as a dynamical object, we identify rank loss as a structural transition that precedes and complements classical indicators of instability. Rank loss enforces spectral concentration, limits calibration transportability, and signals the emergence of coherence in systems ranging from simple maps to turbulent flows.

The framework is general, requiring only differentiability of the forward map and a noise model. It unifies diverse phenomena—early-warning signals, coherent structures, and model breakdown—under a single information-theoretic principle. This suggests that inferability, rather than trajectory divergence, may be the fundamental quantity governing transitions in complex dynamical systems.

References

[1] S. Amari and H. Nagaoka. *Methods of Information Geometry.* American Mathematical Society, 2000.

[2] N. Ay, J. Jost, H. Lê, and L. Schwachhöfer. *Information Geometry.* Springer, 2017.

[3] B. R. Frieden. *Science from Fisher Information.* Cambridge University Press, 2004.

[4] R. S. Ingarden, A. Kossakowski, and M. Ohya. *Information Dynamics and Open Systems.* Springer, 1982.

[5] A. Caticha. Information and entropy in physics. In *Bayesian Inference and Maximum Entropy Methods*, 2007.

[6] D. C. Brody. Information geometry of dynamical systems. *Journal of Physics A*, 45(2):023001, 2012.

[7] E. Ott. *Chaos in Dynamical Systems.* Cambridge University Press, 2002.

[8] S. H. Strogatz. *Nonlinear Dynamics and Chaos.* CRC Press, 2018.

[9] S. Wiggins. *Introduction to Applied Nonlinear Dynamical Systems and Chaos.* Springer, 2003.

[10] M. Scheffer et al. Early-warning signals for critical transitions. *Nature*, 461:53–59, 2009.

[11] V. Dakos et al. Methods for detecting early warnings of critical transitions. *PLoS One*, 7(7):e41010, 2012.

[12] M. B. Giles and N. A. Pierce. An introduction to the adjoint approach to design. *Flow, Turbulence and Combustion*, 65:393–415, 2000.

[13] T. Bewley. DNS-based sensitivity analysis of turbulent flows. *Annual Review of Fluid Mechanics*, 33:335–378, 2001.

[14] U. Frisch. *Turbulence*. Cambridge University Press, 1995.

[15] S. B. Pope. *Turbulent Flows*. Cambridge University Press, 2000.

[16] A. N. Kolmogorov. The local structure of turbulence in incompressible viscous fluid. *Dokl. Akad. Nauk SSSR*, 30:299–303, 1941.

[17] I. Mezić. Spectral properties of dynamical systems, model reduction and coherence. *Physica D*, 197:101–133, 2004.

[18] S. L. Brunton and J. N. Kutz. *Modern Koopman Theory for Dynamical Systems*. Springer, 2022.

[19] R. M. May. Simple mathematical models with very complicated dynamics. *Nature*, 261:459–467, 1976.